Hierarchical Quantum Control Gates for Functional MRI Understanding

Xuan-Bac Nguyen[1,*], Hoang-Quan Nguyen[1,*], Hugh Churchill[2,*], Samee U. Khan[3], Khoa Luu[1,*]

[1] CVIU Lab, University of Arkansas, AR 72703   [2] Dept. of Physics, University of Arkansas, AR 72703

[3] Mississippi State University, MS 39762

* MonArk NSF Quantum Foundry

{xnguyen,hn016,hchurch,khoaluu}@uark.edu, skhan@ece.msstate.edu,

Abstract—Quantum computing has emerged as a powerful tool for solving complex problems intractable for classical computers, particularly in popular fields such as cryptography, optimization, and neurocomputing. In this paper, we present a new quantum-based approach named the Hierarchical Quantum Control Gates (HQCG) method for efficient understanding of Functional Magnetic Resonance Imaging (fMRI) data. This approach includes two novel modules: the Local Quantum Control Gate (LQCG) and the Global Quantum Control Gate (GQCG), which are designed to extract local and global features of fMRI signals, respectively. Our method operates end-to-end on a quantum machine, leveraging quantum mechanics to learn patterns within extremely high-dimensional fMRI signals, such as 30,000 samples—a challenge for classical computers. Empirical results demonstrate that our approach significantly outperforms classical methods. Additionally, we found that the proposed quantum model is more stable and less prone to overfitting than the classical methods.

Index Terms—Quantum Control Gates, Quantum Computer, fMRI, Brain-inspired Representation

I. INTRODUCTION

Brain-inspired representations provide a promising pathway for enhancing the training of deep neural networks (DNN) [1]. To understand these representations, it is crucial to monitor the activities of every single neuron in the brain simultaneously. Among several neurocomputing techniques such as functional Magnetic Resonance Imaging (fMRI), Magnetoencephalography (MEG), and electroencephalogram (EEG), due to the efficiency, it is worth mentioning fMRI signals that have been used widely for that purpose in most recent studies [2]–[15]. These studies explored patterns of fMRI signals in a trivial approach, i.e., using a fully connected layer to extract the features. Meanwhile, understanding the pattern of fMRI signals aims to discover the relationship between neurons that activate together. For instance, when a human perceives a visual science that contains the face of someone, the voxels within *floc-face* region inside the brain will be fired or activated. For that reason, the previous approaches fall apart in exploring fMRI patterns.

Recently, the self-attention mechanism [16] has been a well-known approach to Natural Language Processing (NLP) and has been widely applied across research fields such as computer vision, signal processing, etc [17]–[23]. This mechanism allows a neural network to focus on different parts of the input sequence when processing each element. This mechanism enables the network to weigh the importance of different tokens, i.e., words, subwords, etc., in the input sequence differently, depending on the context. Therefore, using the self-attention mechanism for fMRI signals is a potential approach. In particular, if we treat fMRI signals as an input sequence, the self-attention mechanism automatically measures the voxels-wide correlation inside the signals. A higher correlation means a higher chance that two or more voxels will activate together.

The limitations when using self-attention to deal with very long sequences are high memory and complexity. Especially, the complexity and memory are quadratic and square of the sequence length. Meanwhile, fMRI signals are extremely high-dimensional signals that contain thousands of voxel activations. Thus, utilizing the self-attention mechanism for understanding fMRI signals is still a big obstacle.

Apart from classical computers, quantum computers can process information in parallel thanks to qubits' properties. Specifically, quantum bits, or qubits, can exist in a superposition of states, representing both 0 and 1 simultaneously. It allows a quantum computer to process a vast number of possible outcomes simultaneously, unlike classical bits, which are either 0 or 1. Due to superposition, a quantum computer can evaluate many possible solutions at once. Inspired by this property, we propose a quantum-based solution named a novel approach for fMRI understanding. The Fig. 1 demonstrates the idea of our proposed method. The contributions in this paper can be summarized as follows: (1) We introduce a novel quantum-based solution named Hierarchical Quantum Control Gate (HQCG) for fMRI understanding. This method can learn both local and global information of the signals in parallel. (2) Inspired by controllable gate design, we propose a trainable **local circuit** to explore the **local information** of the fMRI signal. Specifically, this module is a self-attention method that automatically learns the voxel-wise correlations. (3) To learn global information, we gather all local information extracted by **local circuits** and learn pair-wise relationships between this information by using a **global circuit**. (4) From experimental results, the proposed method performs better than a similar one running on a classical computer. Surprisingly, HQCG also helps to prevent overfitting than classical ones.
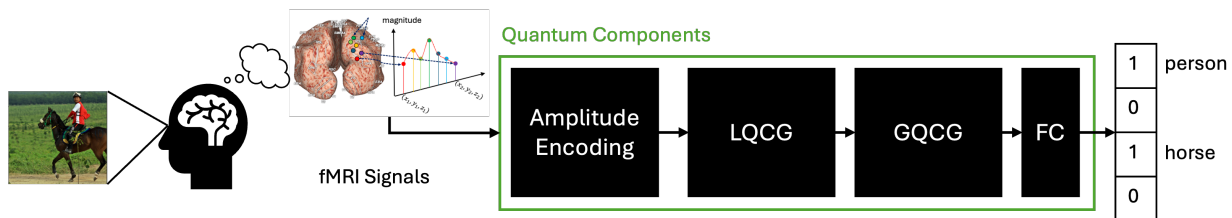
Fig. 1: An overall quantum system for the Functional MRI classification. The green box includes components that run on the quantum computer: Amplitude encoding, Local Quantum Control Gate (LQCG), Global Quantum Control Gate (GQCG), and Fidelity Circuit (FC).

II. BACKGROUND AND RELATED WORK

A. Brain Signal Encoding

Decoding human brain representation has been one of the most popular research topics for a decade. In particular, cognitive neuroscience has made substantial advances in understanding neural representations originating in the primary Visual Cortex (V1) [24]. Indeed, the primary visual context is in response to processing information related to oriented edges and colors. The V1 forwards the information to other neural regions, focusing more on complex shapes and features. These regions are overlapped mainly with receptive fields such as V4 [25], before converging on object and category representations in the inferior temporal (IT) cortex [26]. Neuroimaging techniques, including Functional Magnetic Resonance Imaging (fMRI), Magnetoencephalography (MEG), and electroencephalogram (EEG), have been crucial approaches to these studies. However, to replicate human-level neural representations that fully capture our visual processes, it is crucial to *precisely monitor the activity of every neuron in the brain simultaneously*. Consequently, recent efforts in brain representation decoding have focused on exploring the correlation between neural activity data and computational models. In this research direction, several studies [2]–[6] were presented to decode brain information. Recently, with the help of deep learning, the authors in [7]–[12] presented the methods to reconstruct what humans see from fMRI signal using diffusion models. The authors in [7], [27] also explored patterns of fMRI signals. However, they often need to demonstrate or explain the nature of these patterns.

B. Quantum Basics

A quantum bit or qubit is the information carrier in the quantum computing and communication channel. A qubit is a two-dimensional Hilbert space with two orthonormal bases $|0\rangle$ and $|1\rangle$. These computational bases are usually represented as vectors $|0\rangle = [1, 0]^\top$ and $|1\rangle = [0, 1]^\top$. Due to the unique qubit characteristic of superposition, the state of a qubit can be represented as the sum of two computational bases weighted by complex amplitudes as $|\psi\rangle = \alpha|0\rangle + \beta|1\rangle$, where α and $\beta \in \mathbb{C}$, and $|\alpha|^2 + |\beta|^2 = 1$. $|\alpha|^2$ and $|\beta|^2$ are the probability of obtaining states $|0\rangle$ and $|1\rangle$ after multiple measurements, respectively. It gives an advantage in quantum computing over classical computing when the qubits can be entangled. The two qubits q_0 and q_1 are entangled when they have a state that cannot be individually represented as a complex scalar

times the basis vector. A quantum state $|\psi\rangle$ can be transformed to another state $|\psi'\rangle$ through a quantum circuit represented by a unitary matrix U. The quantum state transformation can be mathematically formulated as $|\psi'\rangle = U|\psi\rangle$. To get classical information from a quantum state $|\psi'\rangle$, quantum measurements are applied by computing the expectation value $\langle H \rangle = \langle \psi'|H|\psi'\rangle$ of a Hermitian matrix H.

C. Parameterized Quantum Circuit

The parameterized quantum circuit (PQC) [28] is a unique quantum circuit with learnable parameters. The PQC includes three modules, i.e., data encoding, parameterized layer, and quantum measurements.

Given a classical data $\mathbf{x} \in \mathbb{R}^D$ where D is the data dimension, the data encoding circuit $U(\mathbf{x})$ is used to transform $\mathbf{x}$ into a quantum state $|\psi\rangle$. The quantum state $|\psi\rangle$ is transformed via parameterized circuits $V(\theta)$ to a new state $|\psi\rangle$. The parameterized circuits is a sequence of quantum circuit operators with learnable parameters denoted as:

$$V(\theta) = V_L(\theta_L)V_{L-1}(\theta_{L-1})\ldots V_1(\theta_1) \qquad (1)$$

where L is the number of operators. The quantum measurements H are used to retrieve the values of the quantum state for further processing. PQC uses a hybrid quantum-classical procedure to optimize the trainable parameters iteratively. The popular optimization approaches include gradient descent [29], parameter-shift rule [30], [31], and gradient-free techniques [32], [33]. Despite various PQC training and inference problems [34]–[37], the PQC poses a potential approach for deep learning tasks in quantum settings due to its entanglement and superposition properties [38], [39].

III. PROPOSED APPROACH

A. Data Encoding

Classical computers operate with bits representing either 0 or 1. In contrast, quantum computers use quantum bits, or qubits, which can exist in superpositions of states, such as $|0\rangle$, $|1\rangle$, or any quantum superposition $\alpha|0\rangle + \beta|1\rangle$. To leverage the computational power of quantum machines, classical data must be transformed into these quantum states. Currently, there are several approaches for quantum data encoding, such as amplitude, phase, or PQC-based encoding (e.g., U_3). In this paper, we utilize the amplitude encoding strategy for the following reasons. First, amplitude encoding requires fewer qubits than others. Especially, given an fMRI signal length of l denoted
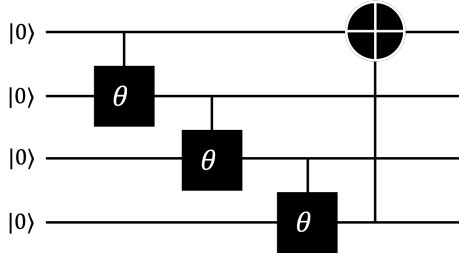
Fig. 2: Local Quantum Control Gate

Fig. 3: Global Quantum Control Gate.

as $v = [v_0, \ldots v_{l-1}] \in \mathbb{R}^l$, the amplitude encoding needs only $\lceil \log_2(l) \rceil$ qubits while phase encoding requires l qubits to encode whole data. Second, the amplitude encoding preserves the natural characteristic of the fMRI signals. In particular, the response of the voxel demonstrates the contribution of this voxel to the processes of the brain. For example, given i^{th} and j^{th} voxel, the expression of $v_i > v_j$ means the ith voxel is more informative than j^{th} voxel. For that reason, amplitude encoding is the most suitable for encoding the fMRI signal.

B. Local Quantum Control Gate

In fMRI signals, nearby voxels exhibit similar responses. Inspired by this observation, we propose a Local Quantum Control Gate (LQCG) to extract local features from fMRI signals. The design of LQCG is illustrated in Fig 2. We group continuous qubits into the LQCG, where two adjacent qubits are entangled using a trainable control unitary operation denoted as θ. The output of this operation is then entangled with the next qubit. Finally, a skip connection is created by aggregating the last entangled information with the first one. The proposed design helps to combine different pieces of information, enhancing the representational power of the LQCG. In self-attention mechanisms, each element in the sequence can attend to every other element, creating a set of attention scores that influence the representation of each element. Similarly, the entanglement in LQCG leads to non-local correlations between qubits. Therefore, the entanglement design can have a similar effect as the self-attention mechanism.

C. Global Quantum Control Gate

As described in the previous section, we have introduced the Local Quantum Control Gate (LQCG) to extract local features from fMRI signals. To extract global features, we propose a novel approach called the Global Quantum Control Gate (GQCG). An overview of GQCG is shown in Fig 3. The concept of GQCG is similar to that of LQCG, incorporating hierarchical trainable control unitary operations θ and skip connections at the end. However, the critical difference is that GQCG uses the output of LQCG as its input and performs pair-wise entanglements between multiple local features. This design enables the aggregation of information from local voxels, providing a comprehensive description of the fMRI signals.

D. Multi-Classification Quantum State Fidelity Circuit

For the classification task, we introduce a multiple quantum state fidelity circuit to classify the quantum state. In detail,
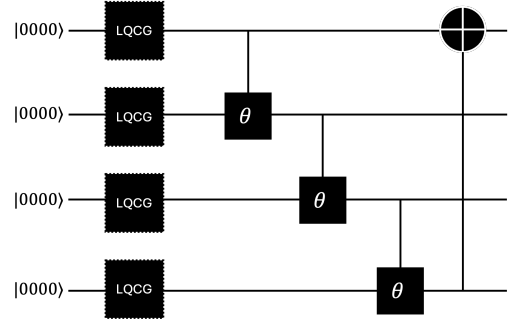
given a quantum state $|\psi\rangle$ computed from the LQCG and GQCG, we compute the fidelity of a learnable quantum state $|\phi_i\rangle$ presenting the i-th class. The fidelity of the quantum states is formulated as $\langle \psi | \phi_i \rangle$. To compute the fidelity in the quantum circuit, a swap test design is used similar to [40].

IV. DATASET AND IMPLEMENTATION DETAILS

A. Dataset

We use the Natural Scenes Dataset (NSD) [41], a comprehensive compilation of responses from eight participants obtained through high-quality 7T fMRI scans. Each subject was exposed to approximately 73,000 natural scenes, forming the basis for constructing visual brain encoding models. Since the visual stimulus in this database is a subset of COCO [42], for each sample, visual stimulus (images) has labels of the objects inside and corresponding fMRI response, respectively. The fMRI data contains signals from both the left and right hemispheres. The length of these signals varies across subjects.

B. Implementation Details

Quantum Components. We use the amplitude encoding method to represent the signal in the quantum system and preserve the relative magnitude of the fMRI. The quantum system requires 16 qubits to encode and extract features from the fMRI signal. For simplification, we use one LQCG layer and one GQCG layer. Then, a multiple quantum state fidelity circuit is used for the multi-classification task. For a fair comparison, we employ feed-forward layers with a similar depth to the quantum components in the classical network.

Objective Loss Function. As a multi-class classification problem, we employ standard binary cross-entropy loss function to optimize the quantum networks.

Training Process. We implement the network using the TorchQuantum library [43] to simulate the quantum machine. Since this library uses PyTorch as the backend, we can leverage GPUs to speed up the training process. The models are trained on an A100 GPU with 40GB of memory. The learning rate starts at 0.01 and progressively decreases to zero following the CosineAnnealing policy [44]. The model is trained with a batch size of 64, AdamW [45] optimizer for 30 epochs, with a training time of approximately 5 minutes.

Evaluation Metrics. We use accuracy and Area Under Curve (AUC) as the metrics for the comparison.

TABLE I: Evaluation results on the NSD dataset. We compute the accuracy and area under the ROC curve (AUC) of the predictions on different subjects and hemispheres.

|		Subj01			Subj02			Subj03			Subj04		
		LH	RH	Both	LH	RH	Both	LH	RH	Both	LH	RH	Both
Accuracy	Classical	87.59%	88.07%	87.06%	87.67%	86.96%	86.14%	87.48%	87.68%	87.29%	86.16%	86.36%	85.43%
	Quantum	**88.53%**	**88.98%**	**89.04%**	**88.89%**	**88.62%**	**88.89%**	**88.59%**	**88.58%**	**88.88%**	**87.38%**	**88.17%**	**87.97%**
		Subj05			Subj06			Subj07			Subj08		
		LH	RH	Both	LH	RH	Both	LH	RH	Both	LH	RH	Both
Accuracy	Classical	88.43%	88.66%	87.42%	87.75%	87.71%	86.70%	86.71%	87.28%	86.86%	85.44%	86.11%	84.94%
	Quantum	**89.91%**	**89.85%**	**90.03%**	**88.93%**	**89.32%**	**89.27%**	**88.02%**	**88.68%**	**88.87%**	**87.15%**	**87.58%**	**87.88%**
		Subj01			Subj02			Subj03			Subj04		
		LH	RH	Both	LH	RH	Both	LH	RH	Both	LH	RH	Both
AUC	Classical	88.82%	89.30%	82.14%	88.76%	87.40%	81.23%	86.93%	86.85%	77.70%	85.27%	86.11%	76.25%
	Quantum	**90.42%**	**90.89%**	**91.31%**	**90.34%**	**89.52%**	**90.50%**	**88.86%**	**88.96%**	**89.51%**	**87.72%**	**89.00%**	**88.89%**
		Subj05			Subj06			Subj07			Subj08		
		LH	RH	Both	LH	RH	Both	LH	RH	Both	LH	RH	Both
AUC	Classical	90.20%	90.52%	78.40%	87.50%	88.22%	78.64%	87.31%	88.28%	82.62%	83.84%	84.32%	76.66%
	Quantum	**92.16%**	**92.15%**	**92.58%**	**89.81%**	**90.40%**	**90.73%**	**89.24%**	**90.14%**	**90.47%**	**86.43%**	**87.17%**	**87.55%**
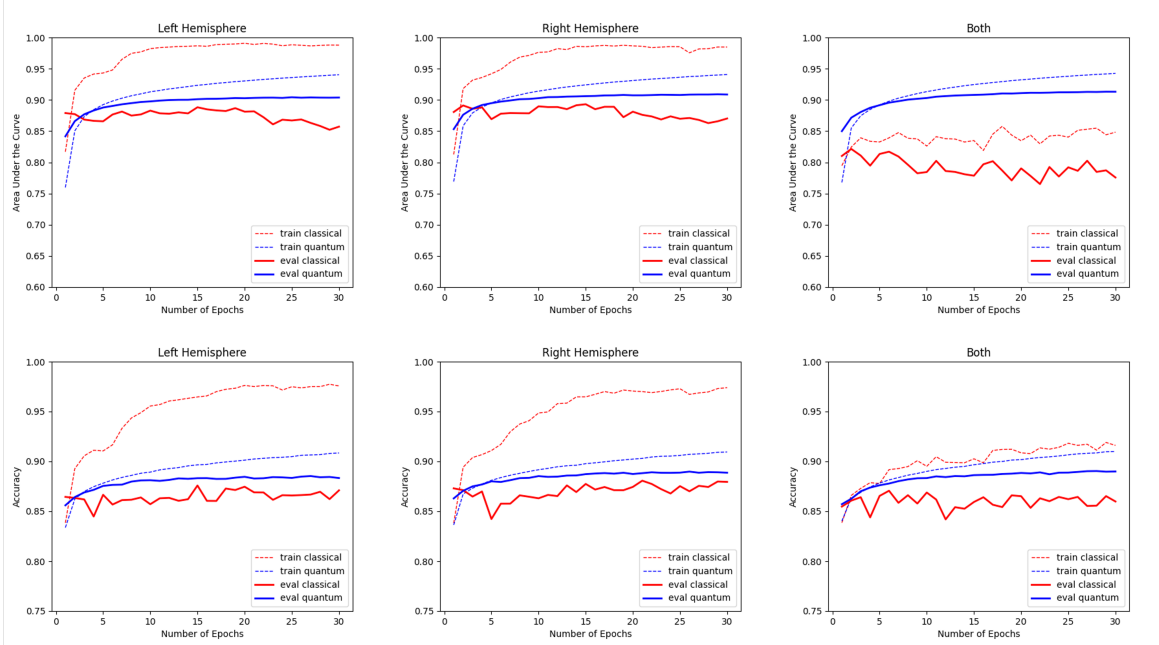
Fig. 4: The training progresses of classical and quantum fMRI classification models using different brain hemispheres, i.e., left hemisphere, right hemisphere, and both.

V. Experiments and Results

A. Multi-Objects Predictions From fMRI

This task aims to predict which objects a participant perceives based on recorded fMRI signals. The dataset includes fMRI signals from both the left and right hemispheres. Table I illustrates the performance of these individual hemispheres and their combination.

Compared to the classical approach, our proposed method achieves approximately 1%-3% higher accuracy for signals from both the left and right hemispheres. Notably, the quantum approach significantly outperforms the classical one when dealing with a combination of signals from both sides of the brain, with an improvement of approximately 8%-14%.

Interestingly, it is clear that for all subjects (from Subj01 to Subj08), the performance of the model running on a classical computer is lower when combining both hemispheres than using either the left or right hemisphere alone. Meanwhile, we observe that the quantum model maintains better performance

than when using signals from just the left or right hemispheres. It can be explained by combining signals from both hemispheres, resulting in a more extended sequence, which challenges the classical approach. In contrast, the quantum approach effectively handles this more extended sequence. This result demonstrates the efficiency of our proposed method and highlights the potential of quantum computing.

B. Training Stability

In this section, we analyze the training stability of the models on classical and quantum computing for fMRI classification problems. We report the accuracy and AUC for both training and validation during the training process, as shown in Fig 4. Initially, when training with the left or right hemispheres, we observe that the training curves of the classical approach are significantly higher than those of the quantum approach; however, the validation curves for the classical approach are consistently lower than those of the quantum approach. It indicates that the classical approach is
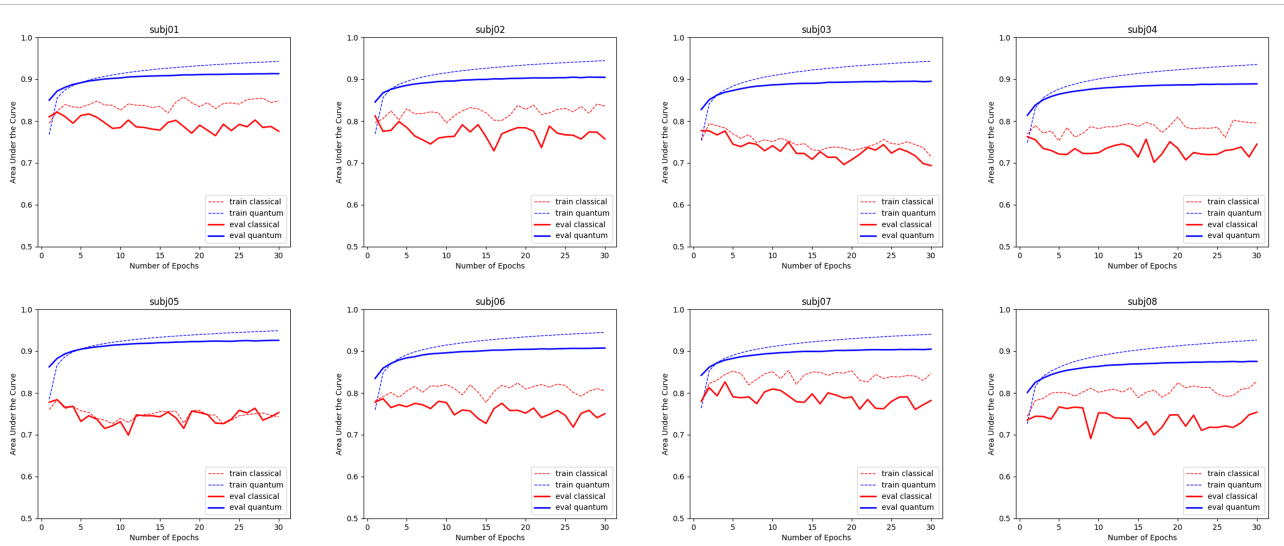
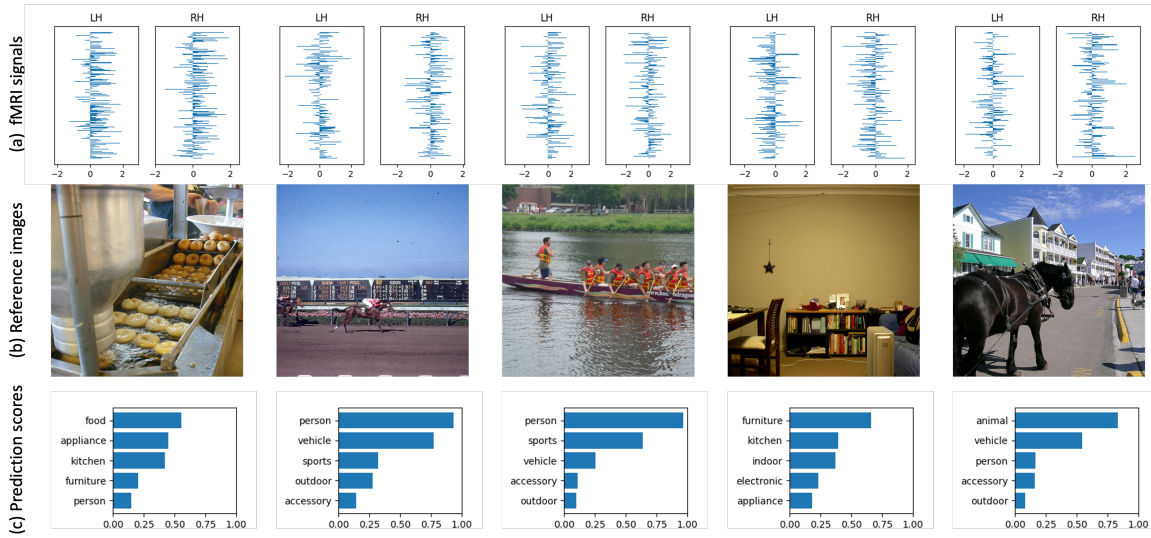Fig. 5: The training progresses of classical and quantum fMRI classification models on different subjects.

Fig. 6: The prediction examples of the proposed HQCG model on the NSD dataset.

more prone to overfitting. Additionally, the classical method's curves exhibit more fluctuations, while the quantum method's curves are stable and smooth, demonstrating greater training stability. In conclusion, the quantum approach can prevent overfitting and stabilize the training process, leading to better results than the classical approach. Fig 5 shows the training progress of classical and quantum models on different subjects. Clearly, our approach's performances and stability consistently perform well on various subjects.

C. Prediction Demonstrations

Fig 6 resents example outputs of our proposed method. Part (a) displays the signals from the left and right hemispheres, part (b) shows the visual stimuli that the subject is viewing, and part (c) illustrates the prediction scores. The prediction bars indicate that our method achieves significantly high confidence scores.

VI. CONCLUSION AND DISCUSSION

In this paper, we present a novel quantum-based method for understanding fMRI data. This method comprises two main components, the Local Quantum Control Gate (LQCG) and the Global Quantum Control Gate (GQCG), designed to learn and extract local and global features from extremely long fMRI signals, such as 30,000 samples. Empirical experiments demonstrate the superior efficiency and stability of our approach on a quantum computer compared to its performance on a classical computer. Implemented to run end-to-end on a quantum machine, our approach leverages quantum mechanics to advance neuroscience and could inspire applications in other fields in the future.

REFERENCES

[1] S. Palazzo, C. Spampinato, I. Kavasidis, D. Giordano, J. Schmidt, and M. Shah, "Decoding brain representations by multimodal learning of neural activity and visual features," *IEEE Transactions on Pattern Analysis and Machine Intelligence*, vol. 43, no. 11, pp. 3833–3849, 2020.

[2] J.-D. Haynes and G. Rees, "Predicting the orientation of invisible stimuli from activity in human primary visual cortex," *Nature neuroscience*, vol. 8, no. 5, pp. 686–691, 2005.

[3] B. Thirion, E. Duchesnay, E. Hubbard, J. Dubois, J.-B. Poline, D. Lebihan, and S. Dehaene, "Inverse retinotopy: inferring the visual content of images from brain activation patterns," *Neuroimage*, vol. 33, no. 4, pp. 1104–1116, 2006.

[4] Y. Kamitani and F. Tong, "Decoding the visual and subjective contents of the human brain," *Nature neuroscience*, vol. 8, no. 5, pp. 679–685, 2005.

[5] D. D. Cox and R. L. Savoy, "Functional magnetic resonance imaging (fmri)"brain reading": detecting and classifying distributed patterns of fmri activity in human visual cortex," *Neuroimage*, vol. 19, no. 2, pp. 261–270, 2003.

[6] J. V. Haxby, M. I. Gobbini, M. L. Furey, A. Ishai, J. L. Schouten, and P. Pietrini, "Distributed and overlapping representations of faces and objects in ventral temporal cortex," *Science*, vol. 293, no. 5539, pp. 2425–2430, 2001.

[7] Z. Chen, J. Qing, T. Xiang, W. L. Yue, and J. H. Zhou, "Seeing beyond the brain: Conditional diffusion model with sparse masked modeling for vision decoding," in *Proceedings of the IEEE/CVF Conference on Computer Vision and Pattern Recognition*, 2023, pp. 22 710–22 720.

[8] P. S. Scotti, A. Banerjee, J. Goode, S. Shabalin, A. Nguyen, E. Cohen, A. J. Dempster, N. Verlinde, E. Yundler, D. Weisberg *et al.*, "Reconstructing the mind's eye: fmri-to-image with contrastive learning and diffusion priors," *arXiv preprint arXiv:2305.18274*, 2023.

[9] Y. Takagi and S. Nishimoto, "High-resolution image reconstruction with latent diffusion models from human brain activity," in *Proceedings of the IEEE/CVF Conference on Computer Vision and Pattern Recognition*, 2023, pp. 14 453–14 463.

[10] F. Ozcelik and R. VanRullen, "Natural scene reconstruction from fmri signals using generative latent diffusion," *Scientific Reports*, vol. 13, no. 1, p. 15666, 2023.

[11] S. Lin, T. Sprague, and A. K. Singh, "Mind reader: Reconstructing complex images from brain activities," *Advances in Neural Information Processing Systems*, vol. 35, pp. 29 624–29 636, 2022.

[12] F. Ozcelik and R. VanRullen, "Brain-diffuser: Natural scene reconstruction from fmri signals using generative latent diffusion," *arXiv preprint arXiv:2303.05334*, 2023.

[13] X.-B. Nguyen, X. Liu, X. Li, and K. Luu, "The algonauts project 2023 challenge: Uark-ualbany team solution," *arXiv preprint arXiv:2308.00262*, 2023.

[14] X.-B. Nguyen, H. Jang, X. Li, S. U. Khan, P. Sinha, and K. Luu, "Bractive: A brain activation approach to human visual brain learning," *arXiv preprint arXiv:2405.18808*, 2024.

[15] X.-B. Nguyen, X. Li, S. U. Khan, and K. Luu, "Brainformer: Modeling mri brain functions to machine vision," *arXiv preprint arXiv:2312.00236*, 2023.

[16] A. Vaswani, N. Shazeer, N. Parmar, J. Uszkoreit, L. Jones, A. N. Gomez, Ł. Kaiser, and I. Polosukhin, "Attention is all you need," *Advances in neural information processing systems*, vol. 30, 2017.

[17] X.-B. Nguyen, D. T. Bui, C. N. Duong, T. D. Bui, and K. Luu, "Clusformer: A transformer based clustering approach to unsupervised large-scale face and visual landmark recognition," in *Proceedings of the IEEE/CVF conference on computer vision and pattern recognition*, 2021, pp. 10 847–10 856.

[18] X.-B. Nguyen, C. N. Duong, X. Li, S. Gauch, H.-S. Seo, and K. Luu, "Micron-bert: Bert-based facial micro-expression recognition," in *Proceedings of the IEEE/CVF Conference on Computer Vision and Pattern Recognition*, 2023, pp. 1482–1492.

[19] H.-Q. Nguyen, T.-D. Truong, X. B. Nguyen, A. Dowling, X. Li, and K. Luu, "Insect-foundation: A foundation model and large-scale 1m dataset for visual insect understanding," in *Proceedings of the IEEE/CVF Conference on Computer Vision and Pattern Recognition*, 2024, pp. 21 945–21 955.

[20] X.-B. Nguyen, G. S. Lee, S. H. Kim, and H. J. Yang, "Self-supervised learning based on spatial awareness for medical image analysis," *IEEE Access*, vol. 8, pp. 162 973–162 981, 2020.

[21] X. B. Nguyen, A. Bisht, H. Churchill, and K. Luu, "Two-dimensional quantum material identification via self-attention and soft-labeling in deep learning," *arXiv preprint arXiv:2205.15948*, 2022.

[22] B. Nguyen-Xuan and G.-S. Lee, "Sketch recognition using lstm with attention mechanism and minimum cost flow algorithm," *International Journal of Contents*, vol. 15, no. 4, pp. 8–15, 2019.

[23] X.-B. Nguyen, C. N. Duong, M. Savvides, K. Roy, H. Churchill, and K. Luu, "Fairness in visual clustering: A novel transformer clustering approach," *arXiv preprint arXiv:2304.07408*, 2023.

[24] K. J. Seymour, M. A. Williams, and A. N. Rich, "The representation of color across the human visual cortex: distinguishing chromatic signals contributing to object form versus surface color," *Cerebral cortex*, vol. 26, no. 5, pp. 1997–2005, 2016.

[25] J. W. Peirce, "Understanding mid-level representations in visual processing," *Journal of Vision*, vol. 15, no. 7, pp. 5–5, 2015.

[26] I. T. Cortex, "Fast readout of object identity from macaque," *science*, vol. 1117593, no. 863, p. 310, 2005.

[27] P. Y. Kim, J. Kwon, S. Joo, S. Bae, D. Lee, Y. Jung, S. Yoo, J. Cha, and T. Moon, "Swift: Swin 4d fmri transformer," *arXiv preprint arXiv:2307.05916*, 2023.

[28] M. Benedetti, E. Lloyd, S. Sack, and M. Fiorentini, "Parameterized quantum circuits as machine learning models," *Quantum Science and Technology*, vol. 4, no. 4, p. 043001, 2019.

[29] R. Sweke, F. Wilde, J. Meyer, M. Schuld, P. K. Fährmann, B. Meynard-Piganeau, and J. Eisert, "Stochastic gradient descent for hybrid quantum-classical optimization," *Quantum*, vol. 4, p. 314, 2020.

[30] D. Wierichs, J. Izaac, C. Wang, and C. Y.-Y. Lin, "General parameter-shift rules for quantum gradients," *Quantum*, vol. 6, p. 677, 2022.

[31] K. Mitarai, M. Negoro, M. Kitagawa, and K. Fujii, "Quantum circuit learning," *Physical Review A*, vol. 98, no. 3, p. 032309, 2018.

[32] G. Nannicini, "Performance of hybrid quantum-classical variational heuristics for combinatorial optimization," *Physical Review E*, vol. 99, no. 1, p. 013304, 2019.

[33] S. Y.-C. Chen, C.-M. Huang, C.-W. Hsing, H.-S. Goan, and Y.-J. Kao, "Variational quantum reinforcement learning via evolutionary optimization," *Machine Learning: Science and Technology*, vol. 3, no. 1, p. 015025, 2022.

[34] J. R. McClean, S. Boixo, V. N. Smelyanskiy, R. Babbush, and H. Neven, "Barren plateaus in quantum neural network training landscapes," *Nature communications*, vol. 9, no. 1, p. 4812, 2018.

[35] X.-B. Nguyen, H.-Q. Nguyen, H. Churchill, S. U. Khan, and K. Luu, "Quantum visual feature encoding revisited," *arXiv preprint arXiv:2405.19725*, 2024.

[36] H.-Q. Nguyen, X. B. Nguyen, S. Y.-C. Chen, H. Churchill, N. Borys, S. U. Khan, and K. Luu, "Diffusion-inspired quantum noise mitigation in parameterized quantum circuits," *arXiv preprint arXiv:2406.00843*, 2024.

[37] X. B. Nguyen, B. Thompson, H. Churchill, K. Luu, and S. U. Khan, "Quantum vision clustering," *arXiv preprint arXiv:2309.09907*, 2023.

[38] X.-B. Nguyen, H.-Q. Nguyen, S. Y.-C. Chen, S. U. Khan, H. Churchill, and K. Luu, "Qclusformer: A quantum transformer-based framework for unsupervised visual clustering," *arXiv preprint arXiv:2405.19722*, 2024.

[39] S. Y.-C. Chen, C.-H. H. Yang, J. Qi, P.-Y. Chen, X. Ma, and H.-S. Goan, "Variational quantum circuits for deep reinforcement learning," *IEEE access*, vol. 8, pp. 141 007–141 024, 2020.

[40] H. Buhrman, R. Cleve, J. Watrous, and R. De Wolf, "Quantum fingerprinting," *Physical review letters*, vol. 87, no. 16, p. 167902, 2001.

[41] E. J. Allen, G. St-Yves, Y. Wu, J. L. Breedlove, J. S. Prince, L. T. Dowdle, M. Nau, B. Caron, F. Pestilli, I. Charest *et al.*, "A massive 7t fmri dataset to bridge cognitive neuroscience and artificial intelligence," *Nature neuroscience*, vol. 25, no. 1, pp. 116–126, 2022.

[42] T.-Y. Lin, M. Maire, S. Belongie, J. Hays, P. Perona, D. Ramanan, P. Dollár, and C. L. Zitnick, "Microsoft coco: Common objects in context," in *Computer Vision–ECCV 2014: 13th European Conference, Zurich, Switzerland, September 6-12, 2014, Proceedings, Part V 13*. Springer, 2014, pp. 740–755.

[43] H. Wang, Y. Ding, J. Gu, Z. Li, Y. Lin, D. Z. Pan, F. T. Chong, and S. Han, "Quantumnas: Noise-adaptive search for robust quantum circuits," in *The 28th IEEE International Symposium on High-Performance Computer Architecture (HPCA-28)*, 2022.

[44] I. Loshchilov and F. Hutter, "Sgdr: Stochastic gradient descent with warm restarts," *arXiv preprint arXiv:1608.03983*, 2016.

[45] ——, "Decoupled weight decay regularization," *arXiv preprint arXiv:1711.05101*, 2017.